Three-Dimensional Invisibility Cloak at Optical Wavelengths

Tolga Ergin,[1,2]*† Nicolas Stenger,[1,2]* Patrice Brenner,[2] John B. Pendry,[3] Martin Wegener[1,2,4]

We have designed and realized a three-dimensional invisibility-cloaking structure operating at optical wavelengths based on transformation optics. Our blueprint uses a woodpile photonic crystal with a tailored polymer filling fraction to hide a bump in a gold reflector. We fabricated structures and controls by direct laser writing and characterized them by simultaneous high–numerical-aperture, far-field optical microscopy and spectroscopy. A cloaking operation with a large bandwidth of unpolarized light from 1.4 to 2.7 micrometers in wavelength is demonstrated for viewing angles up to 60°.

As today's nanofabrication capabilities continue to improve, we are better able to address the inverse problem of electromagnetism with respect to what nanostructure will perform a requested functionality. In this regard, transformation optics (*1*–*14*) is a unique and intuitive scientific tool that allows for the mathematical mapping of desired distortions of space onto an actual distribution of optical material properties in normal Cartesian space. Tailored inhomogeneous metamaterials enable us to approximate these target distributions. Invisibility-cloaking structures (*1*–*16*) can serve as benchmark examples for the much broader ideas of transformation optics.

[1]Institut für Angewandte Physik, Karlsruhe Institute of Technology (KIT), D-76128 Karlsruhe, Germany. [2]DFG–Center for Functional Nanostructures, KIT, D-76128 Karlsruhe, Germany. [3]Blackett Laboratory, Imperial College London, London SW7 2AZ, UK. [4]Institut für Nanotechnologie, KIT, D-76021 Karlsruhe, Germany.

*These authors contributed equally to this work.
†To whom correspondence should be addressed. E-mail: tolga.ergin@kit.edu

So far, invisibility-cloaking experiments at microwave (*5*, *10*) and optical frequencies (*11*–*14*) have been performed exclusively in two-dimensional (2D) waveguide geometries. In other words, these structures are immediately visible from the third dimension. Cloaking works only in the plane; the viewing angle is effectively zero in one direction. Nevertheless, these structures have supported the validity of the concepts of both transformation optics and metamaterials.

We designed, fabricated, and characterized 3D invisibility-cloaking structures using tailored, dielectric face-centered–cubic (fcc) woodpile photonic crystals. We studied the behavior of these structures from wavelengths near the woodpile rod spacing (where the onset of diffraction of light leads to the Wood or Rayleigh anomaly in transmittance and reflectance) up to wavelengths much larger than this spacing (the effective-medium limit).

In the carpet-cloak geometry (*8*, *10*–*13*), a bump in a metallic mirror is hidden by adding a tailored refractive-index distribution on top. This distribution can be calculated using the rules of transformation optics (*8*, *10*). Though originally designed for two dimensions, it has been shown (by numerical rendering of photorealistic images via ray tracing) that the carpet-cloak concept should also work in a truly 3D setting and also for very large viewing angles (*17*). In our 3D blueprint (Fig. 1A), the bump is translationally invariant along the z direction and follows $y(x) = h\cos^2(\pi x/w)$ for $|x| \le w/2$ and zero otherwise. Here, $h = 1$ μm is the height of the bump, and $w = 13$ μm is its full width. For the quasi-conformal mapping of the cloak, we choose a width of 26 μm in the x direction and 10 μm in the y direction. This cloak is surrounded by a homogeneous woodpile structure, which is characterized in fig. S5 (*18*). Inside the cloak, the local effective refractive index is controlled via the volume filling fraction (f) of the polymer serving as constituent material for a usual woodpile photonic crystal (*19*, *20*). The diamond-symmetry woodpile geometry is chosen because it is expected to lead to nearly isotropic optical properties. The effective refractive index becomes $n = 1.52$ for $f = 1$ (bulk polymer) and $n = 1.00$ for $f = 0$ (air void). For intermediate values of f, we used the Massachusetts Institute of Technology Photonics-Bands package (*21*) to evaluate the effective local refractive index (Fig. 1B) on the basis of usual photonic-band–structure calculations. We found that the calculated 3D isofrequency contours are very nearly spherical in the long-wavelength limit (see inset in Fig. 1B).

Figure 2 shows the target refractive-index distributions obtained from the quasi-conformal mapping (*8*) and corresponding electron micrographs of some of our structures made by standard direct laser writing lithography (*20*, *22*).

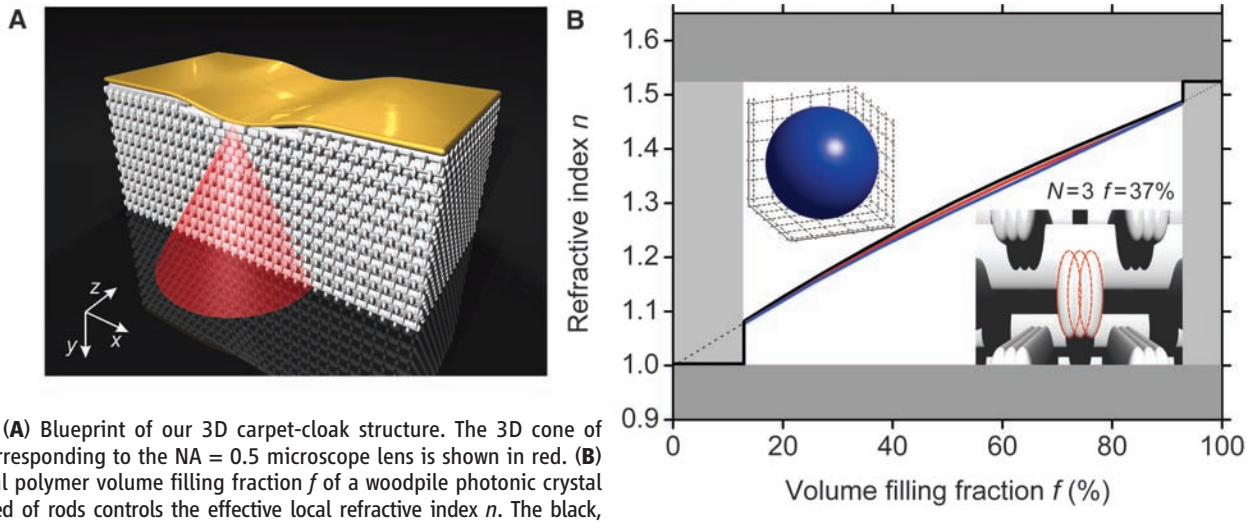

Fig. 1. (**A**) Blueprint of our 3D carpet-cloak structure. The 3D cone of light corresponding to the NA = 0.5 microscope lens is shown in red. (**B**) The local polymer volume filling fraction f of a woodpile photonic crystal composed of rods controls the effective local refractive index n. The black, red, and blue curves correspond to rod aspect ratios (= height/width) of 1, 2, and 3, respectively. The polymer needs to be connected, as do the air voids. These conditions impose lower and upper bounds on f, shown here for a rod aspect ratio of 2. The range of accessible values of n is restricted to be within 1.00 (air) and 1.52 (bulk polymer). The filling fraction is actually controlled by the number of voxels ($N \in \{0,3,4,5,6\}$) that each rod is composed of. The case of $N = 3$ is illustrated by the inset in the lower right corner. For this case and for a vacuum wavelength of 2.4 μm and a rod spacing of 0.8 μm, the upper left inset depicts the nearly spherical isofrequency surface in wave-vector space.

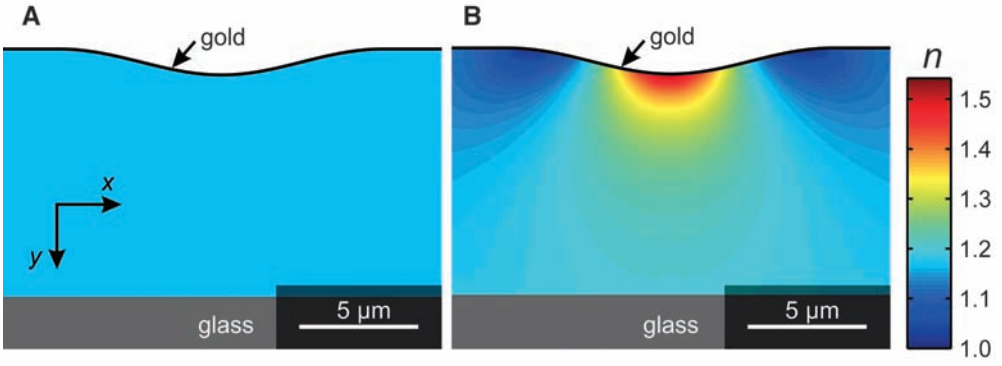

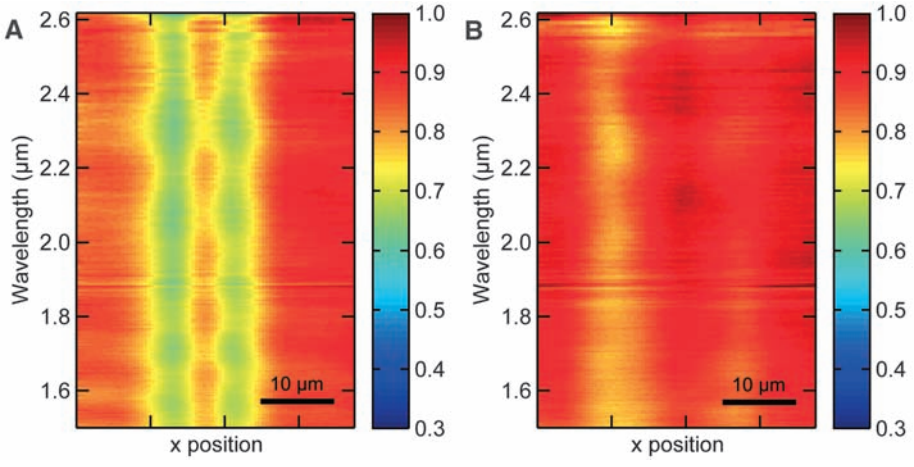

Fig. 2. Target refractive index (n) distributions (top) and oblique-view electron micrographs of fabricated structures after FIB milling (bottom). (**A**) A bump without a cloak. (**B**) A bump with a cloak. Note that the oblique view in the electron micrographs compresses the y direction.

Fig. 3. Optical characterization of the 3D structures (see Fig. 2) with unpolarized light in bright-field mode. The image intensity is shown on a false-color scale. The horizontal axis is a cut through the middle of the structure along the x direction (compare to Fig. 1A); the vertical axis is wavelength. (**A**) A bump without a cloak. The bump is immediately visible. (**B**) Result for a bump with a cloak that approaches the expectation for an ideal cloak (constant intensity).

Fabrication details and sample dimensions are reported in the supporting online material (SOM) (*18*). To reveal their interiors, the structures are cut by means of focused ion beam (FIB) milling. This destructive measure is of utmost importance, as inspection of sample edges can be highly misleading due to the proximity effect.

For what wavelengths do we expect reasonable cloaking? On one hand, it is sometimes argued that the wavelength of light needs to be at least one order of magnitude larger than the period or lattice constant to truly reach the effective-medium limit. This very conservative estimate would lead to operation wavelengths larger than 8 μm for a = 800 nm or a wavelength of 11 μm for the fcc lattice constant of 1.131 μm. On the other hand, the most aggressive and optimistic approach is to argue that the effective-medium method can work up to the Wood anomaly. Once diffraction occurs, the periodic structure can no longer be considered a homogeneous effective material. For normal incidence, diffraction of light becomes possible if the material wavelength is equal to or smaller than the lattice constant. For a = 0.8 μm and a glass-substrate refractive index of n = 1.5, the Wood anomaly is expected to occur at a vacuum wavelength of 1.2 μm. These conservative and aggressive considerations obviously differ by about one order of magnitude in wavelength.

To evaluate the performance of our fabricated samples, we start by discussing the results obtained by bright-field optical microscopy and spectroscopy. The numerical aperture (NA) of the used microscope lens of NA = 0.5 is equivalent to a full opening angle of the cone of light of 60° (Fig. 1A). Therefore, light is propagating not only in the xy plane (which would merely be 2D), but also in oblique directions (3D). Details of the home-built setup are described in the SOM (*18*). Corresponding spatially and spectrally resolved normal-incidence data (normalized) show that the bump is immediately visible by two pronounced spatial minima (Fig. 3A) resulting from light that is reflected by the two slopes of the bump toward the sides and is not collected by the lens. The light reflected from the top of the bump (where the tangent is horizontal) leads to the narrow bright stripe in the middle. The spectral oscillations are Fabry-Perot fringes. Their free spectral range agrees well with the expectation based on the total 10-μm thickness of the woodpile structure. In presence of the cloak and bump (Fig. 3B), the visibility of the bump is strongly suppressed, whereas cloaking is not quite perfect. This recovery works well in the depicted wavelength range of 1.5 to 2.6 μm in Fig. 3 (data over a larger spectral interval are shown in fig. S1). For wavelengths shorter than ~1.2 μm, the image becomes dimmer. Furthermore and most important, in this regime, no recovery due to the presence of the cloak is observed. We interpret this short-wavelength dark region as being due to the Wood anomaly. Indeed, an ideal polymer woodpile can diffract as much as 50% of the incident light for wavelengths smaller than the Wood anomaly (see fig. S5). These levels explain the findings of our present work. For wavelengths shorter than that of the Wood anomaly, the light field can no longer effectively average over the nanostructure. Hence, the structure is not expected to act like a locally homogeneous dielectric, and no cloaking action is expected—consistent with our above observations. For the present conditions, the effective-medium approximation turns out to be much more forgiving than one might be tempted to believe at first sight.

Control samples with only (i) the high-index region or (ii) the two low-index regions are shown in figs. S2 and S3, respectively. For case (ii), the bump appears wider than in Fig. 3A. For case (i), cloaking is worse than for the complete cloak in Fig. 3B. These two observations show that one really needs the complete refractive-index profile

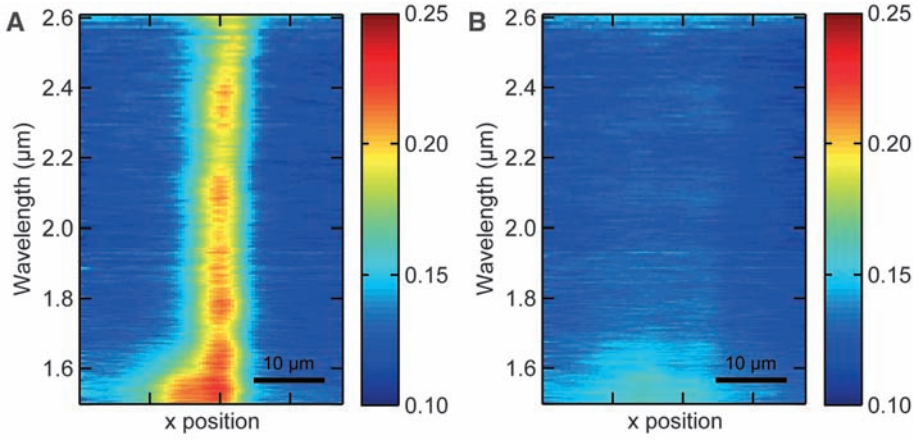

Fig. 4. Optical characterization of the 3D structures with unpolarized light as in Fig. 3, but in dark-field mode. (**A**) The bump is immediately visible by enhanced scattering. (**B**) Scattering is largely reduced with the cloak.

derived from the quasi-conformal mapping in transformation optics to obtain good invisibility-cloaking performance.

Finally, Fig. 4 depicts data taken in dark-field mode from 1.5- to 2.6-μm wavelengths (data over a larger spectral interval are shown in fig. S4). Here, the same sample as in Fig. 3 is tilted such that the optical axis lies within the *xy* plane and includes an angle of 35° with the *y* axis. As usual for the dark-field mode, the collected light results from scattering by the sample. These data are normalized with respect to a normal-incidence reflection spectrum taken on the gold film. The bump without cloak in Fig. 4A is immediately visible. We assign this finding to enhanced scattering from the illuminated side of the bump. The visibility is again drastically reduced for the case of bump with cloak in Fig. 4B.

References and Notes

1. J. B. Pendry, D. Schurig, D. R. Smith, *Science* **312**, 1780 (2006); published online 25 May 2006 (10.1126/science.1125907).
2. U. Leonhardt, *Science* **312**, 1777 (2006); published online 25 May 2006 (10.1126/science.1126493).
3. U. Leonhardt, T. G. Philbin, *New J. Phys.* **8**, 247 (2006).
4. U. Leonhardt, *New J. Phys.* **8**, 118 (2006).
5. D. Schurig *et al.*, *Science* **314**, 977 (2006); published online 19 October 2006 (10.1126/science.1133628).
6. W. Cai, U. K. Chettiar, A. V. Kildishev, V. M. Shalaev, *Nat. Photonics* **1**, 224 (2007).
7. V. M. Shalaev, *Science* **322**, 384 (2008).
8. J. Li, J. B. Pendry, *Phys. Rev. Lett.* **101**, 203901 (2008).
9. U. Leonhardt, T. Tyc, *Science* **323**, 110 (2009); published online 20 November 2008 (10.1126/science.1166332).
10. R. Liu *et al.*, *Science* **323**, 366 (2009).
11. J. Valentine, J. Li, T. Zentgraf, G. Bartal, X. Zhang, *Nat. Mater.* **8**, 568 (2009).
12. L. H. Gabrielli, J. Cardenas, C. B. Poitras, M. Lipson, *Nat. Photonics* **3**, 461 (2009).
13. J. H. Lee *et al.*, *Opt. Express* **17**, 12922 (2009).
14. I. I. Smolyaninov, V. N. Smolyaninova, A. V. Kildishev, V. M. Shalaev, *Phys. Rev. Lett.* **102**, 213901 (2009).
15. G. W. Milton, N. A. P. Nicorovici, *Proc. R. Soc. London Ser. A* **462**, 3027 (2006).
16. A. Alù, N. Engheta, *Phys. Rev. E* **72**, 016623 (2005).
17. J. C. Halimeh, T. Ergin, J. Mueller, N. Stenger, M. Wegener, *Opt. Express* **17**, 19328 (2009).
18. See supporting material available on *Science* Online.
19. K. M. Ho, C. T. Chan, C. M. Soukoulis, R. Biswas, M. Sigalas, *Solid State Commun.* **89**, 413 (1994).
20. M. Deubel *et al.*, *Nat. Mater.* **3**, 444 (2004).
21. S. G. Johnson, J. D. Joannopoulos, *Opt. Express* **8**, 173 (2001).
22. S. Kawata, H.-B. Sun, T. Tanaka, K. Takada, *Nature* **412**, 697 (2001).

23. We thank K. Busch, G. von Freymann, S. Linden, and M. Thiel for discussions and help regarding sample fabrication and photonic band-structure calculations. We acknowledge support from the Deutsche Forschungsgemeinschaft (DFG) and the State of Baden-Württemberg through the DFG–Center for Functional Nanostructures within subprojects A1.4 and A1.5. We also thank the Future and Emerging Technologies (FET) program within the Seventh Framework Programme for Research of the European Commission (FET open grant number 213390) for financial support of the project PHOME. The project METAMAT is supported by the Bundesministerium für Bildung und Forschung. The Ph.D. education of T.E. is embedded in the Karlsruhe School of Optics and Photonics (KSOP); N.S. is supported as a mentor in the KSOP.

Supporting Online Material

www.sciencemag.org/cgi/content/full/science.1186351/DC1
SOM Text
Figs. S1 to S5

23 December 2009; accepted 4 March 2010
Published online 18 March 2010;
10.1126/science.1186351
Include this information when citing this paper.

Dilithioplumbole: A Lead-Bearing Aromatic Cyclopentadienyl Analog

Masaichi Saito,[1]* Masafumi Sakaguchi,[1] Tomoyuki Tajima,[1] Kazuya Ishimura,[2] Shigeru Nagase,[2] Masahiko Hada[3]

Although the concept of aromaticity has long played an important role in carbon chemistry, it has been unclear how applicable the stabilizing framework is to the heaviest elements. Here we report the synthesis of dilithiotetraphenylplumbole by reduction of hexaphenylplumbole. X-ray crystallography revealed a planar structure with no alternation of carbon–carbon bond lengths in the five-membered ring core. Nuclear magnetic resonance spectra and relativistic theoretical calculations show considerable aromatic character in the molecule, thus extending aromaticity to carbon's heaviest congener.

Aromaticity has been a fundamental chemical concept since the discovery of benzene in 1825, and aromatic compounds have long played important roles in all fields of chemistry. The skeletons of most aromatic compounds consist of C atoms, and occasionally N, O, and the third-row elements S and more rarely P. To determine whether the heavier group-14 elements could sustain aromaticity, Si and Ge analogs of carbocyclic aromatic compounds such as benzene, naphthalene (*1*, *2*), cyclopentadienyl anion (*3*–*7*), cyclobutadiene dianion (*8*), and cyclopropenyl cation (*9*–*12*) have recently been synthesized, in which one ring C is replaced by the congener. Most of these have considerable aromatic character, even though some of them have been judged nonaromatic because of their nonplanar structures. Most recently, dilithiostannole (*13*) and 2-stannanaphthalene (*14*) have been synthesized and concluded to be aromatic compounds. Therefore, the concept of aromaticity has been expanded to Sn-containing carbocyclic systems. However, there has been no experimental evidence of whether the concept of aromaticity can be expanded to Pb-containing C rings, even though theoretical calculations predicted that dilithioplumbole would have considerable aromatic character (*15*, *16*). We report here the synthesis of dilithiotetraphenylplumbole, thus expanding the concept of aromaticity to C cycles incorporating the heaviest group-14 element (*17*).

The synthesis of dilithiotetraphenylplumbole **1** was accomplished by the reduction of hexa-

[1]Department of Chemistry, Graduate School of Science and Engineering, Saitama University, Shimo-okubo, Sakura-ku, Saitama-city, Saitama, 338-8570 Japan. [2]Department of Theoretical Molecular and Computational Science, Institute for Molecular Science, Myodaiji, Okazaki, Aichi, 444-8585 Japan. [3]Department of Chemistry, Graduate School of Science and Engineering, Tokyo Metropolitan University, Minami-osawa, Hachiohji, Tokyo, 192-0397 Japan.

*To whom correspondence should be addressed. E-mail: masaichi@chem.saitama-u.ac.jp